IET Generation, Transmission & Distribution

Research Article

Optimal placement of battery energy storage in distribution networks considering conservation voltage reduction and stochastic load composition

ISSN 1751-8687
Received on 31st March 2017
Revised 23rd May 2017
Accepted on 24th May 2017
E-First on 5th October 2017
doi: 10.1049/iet-gtd.2017.0508
www.ietdl.org

Yongxi Zhang[1], Shuyun Ren[2], Zhao Yang Dong[3], Yan Xu[4] ✉, Ke Meng[5], Yu Zheng[6]

[1]*School of Electrical and Information Engineering, Changsha University of Science and Technology, Changsha 410114, People's Republic of China*

[2]*Hong Kong Polytechnic University, Kowloon, Hong Kong*

[3]*School of Electrical Engineering and Telecommunication, University of New South Wales, Sydney, NSW 2052, Australia*

[4]*School of Electrical and Electronic Engineering, Nanyang Technological University, 639798 Singapore, Singapore*

[5]*School of Electrical and Information Engineering, University of Sydney, NSW 2006, Australia*

[6]*Electric Power Research Institute, China Southern Power Grid Company, Guangzhou 510080, People's Republic of China*

✉ *E-mail: eeyanxu@gmail.com*

Abstract: Deployment of battery energy storage (BES) in active distribution networks (ADNs) can provide many benefits in terms of energy management and voltage regulation. In this study, a stochastic optimal BES planning method considering conservation voltage reduction (CVR) is proposed for ADN with high-level renewable energy resources. The proposed method aims to determine the optimal BES sizing and location to minimise the total investment and operation cost considering energy saving achieved by CVR, while satisfying system operational constraints in the presence of stochastic renewable power generation. The uncertainty of load composition is also modelled through scenario analysis. The proposed planning scheme is tested in a modified IEEE 15-bus system and 43-bus radial system, respectively. The numerical results validate that the combination of CVR and BES can achieve more energy savings.

1 Introduction

With the increased penetration of distributed generation (DG) nowadays, the traditional distribution system is evolving from passive to active distribution networks (ADNs) [1]. However, the uncertain and uncontrollable nature of intermittent renewable DG (such as wind and photovoltaic – PV) can significantly affect the operation of the distribution system, inducing issues like voltage rise, bi-direction power flow, power flow fluctuations and so on. Energy storage system (ESS) is one of the most effective solutions for alleviating above problems [2] and readily applied in distribution networks for increasing energy efficiency, enhancing power system reliability and stability, relieving peak load demand pressure and balancing supply and demand [2]. Among different types of ESSs, battery energy storage (BES) is the most fast-growing and wide-spread one in distribution networks due to its unique advantages, e.g. high efficiency, easily scaled to residential size, fast response speed and so on. One of the major problems related to BES application to distribution networks is the optimal planning of the BES unit's type, size, and location based on different objectives [3–8]. In these studies, the planning of BES focused on load-management [3], reliability enhancement [4], voltage regulation [5], peak load-shaving [6] and wind power forecast error mitigation [7] and so on. In our previous work [8], an optimal BES planning framework was proposed aiming to reduce wind power curtailment. Besides, a number of methods have been applied for solving the optimal planning problem, such as heuristic algorithms [3, 5, 8], exhaustive search [6] and decomposition method [4]. However, none of these studies considers the potential voltage reduction effects and associated energy saving after the installation of BES.

CVR controls the voltage level in medium/low voltage distribution networks in the lower band of a permissible range to reduce load demand [9]. The implementation of CVR brings numerous benefits for utilities in various aspects including (i) economic benefits: reduced generation cost due to load demand reduction; (ii) technical improvements: extension of transformer lifetime with the diminished iron losses [10]; and (iii) environmental benefits: predictable decline in carbon dioxide emission. The practical CVR test was first performed by American Electric Power System (AEP) in 1973 [9], and being promoted by many utilities and public services all over the world since then. Nowadays with the continuous development of smart grid technologies, especially in real-time measurement, CVR has re-drawn public concern from industry and academia society [11, 12]. In U.S continent, it is reported that the implementation of CVR leads to 3.4% total energy saving for all distribution feeders in annual energy consumption [13]; while in Australia and Hydro-Quebec, 0.4 and 0.68% of energy saving can be obtained via 1.0% of voltage reduction, respectively [14, 15]. Previous CVR tests are conducted using traditional devices such as on-load tap-changing transformers (OLTC), switched capacitors and voltage regulators for voltage regulation [16]. In recent years, the increasing penetration of DG in ADNs also has the potential for CVR implementation. The authors in [17] first combine the concepts of CVR and DG placement together, a two-stage stochastic optimisation framework is proposed to optimise the location and capacities of wind turbine units and PV arrays. Numerical results suggest that more energy savings can be achieved while implementing CVR and DG simultaneously. Quijano and Feltrin [18] made a further investigation of DG impacts with CVR with reactive power control. However, very few consider utilising BES for CVR purpose.

In this paper, we propose a stochastic BES planning method in ADN considering the BES-based CVR for load demand reduction and voltage profile improvement simultaneously. This work assumes that the utility is the solo investor of BES, also is the promoters and beneficiary of CVR scheme. The combined effects of load demand reduction by implementing CVR via adjusting voltage regulation devices and BES are modelled. Furthermore, the impacts of load composition variation on CVR implementation are also considered through scenario analysis. The main contributions of this paper include the following:

i. A new planning model is proposed for BES placement considering the CVR-based energy saving.
ii. Stochastic load composition is modelled to account for realistic CVR impact.
iii. A chance-constraint is added into the model to ensure a certain level of CVR effect.

This paper is structured as follows. The basic concepts of CVR and the static load model are introduced in Section 2. Then, a stochastic BES planning framework considering CVR implementation is proposed in Section 3, the detailed formation of costs functions are presented then. Instead of conventional load model, the static load model is applied for power flow calculation. After that, a modified 15-bus distribution system and 43-bus radial system are applied to verify the effectiveness of the proposed planning method in Section 4, respectively. Conclusions are drawn in Section 5.

2 CVR and load models

2.1 Basic concept of CVR

The principle of CVR is to achieve energy saving by strategically reducing the voltage profile at the distribution feeder, without causing any inconvenience to consumer appliances [19]. In practice, the voltage magnitude can be lowered down to an acceptable level as per the utility requirements. For example, according to IEEE std 1250-1995 [20] and American National Standards Institute (ANSI) std C84.1-2006 [21], the allowable range of voltages at the distribution transformer secondary terminals can be set as ±6% of the nominal value (120 V).

Mathematically, the CVR factor can be expressed as follows:

$$\mathrm{CVR_f} = \frac{\Delta E\%}{\Delta v\%} \tag{1}$$

where $\Delta E\%$ and $\Delta v\%$ refer to the percentages of total energy saving caused by the reduction of voltage of distribution feeder, strategically.

2.2 Exponential load models

The distribution network system takes responsibility for delivering power to every end user by appropriate voltage level [22]. The high-voltage power is converted to medium/low voltage level in the secondary distribution systems. It is worth mentioning that the vast majority of the loads in medium/low voltage distribution network exhibit voltage-dependent behaviour. That is to say, their load demands are highly related to the voltage magnitude. In a distribution system, due to the particular radial structure and large resistance-to-reactance ratio (R/X), the bus voltage is also very sensitive to the active power. Therefore, to accurately model the CVR effect, a detailed load model is necessary. Previous studies [11, 23] use the static load model, such as exponential, polynomial (ZIP) models instead of constant-power load model for power flow calculation. One common feature of these models is: load consumption is expressed as a function of voltage. The author in [24] conducted a series of tests to compare different static load models (mainly residential and commercial loads) for CVR implementation. The results for ZIP load models and exponential models showed equivalent results in most cases. In this work, the exponential load model is applied to evaluate the CVR effects to facilitate computation. Note however that other load model can also be considered if necessary.

The general forms of exponential active/reactive load model are shown as follows:

$$Pl_i = P_{ni}\left(\frac{v_i}{v_n}\right)^{k_p} \tag{2}$$

$$Ql_i = Q_{ni}\left(\frac{v_i}{v_n}\right)^{k_q} \tag{3}$$

where v_i and v_n denote the voltage magnitude at bus i and rated voltage of the system, respectively; Pl_i and Ql_i denote the active and reactive powers of bus i, respectively; P_{ni} and Q_{ni} denote the active and reactive load powers of bus i at the rated voltage, respectively; k_p and k_q denote the exponential parameters for active and reactive powers, respectively. According to comprehensive statistic studies, the load can be categorised into three types: industrial, residential and commercial. Values for the parameters of exponential factors are shown in Table 1.

Table 1 Values of k_p and k_q [19]

Load type	k_p	k_q
residential	1.04	4.19
commercial	1.50	3.15
industrial	0.18	6.00

To accurately model the CVR benefits, the influence of different load types should be considered. Moreover, during practical operation phase, the load composition randomly varies from time to time; therefore it is necessary to take this stochastic load composition into account.

3 Problem formulation and solution technique

The overall objective of the proposed planning model is finding suitable location and capacity of BES to be installed in ADN, aims to minimise the sum of total investment cost, operation & maintenance cost of BES as well as the daily operation cost under different scenarios.

3.1 Objective function

In order to integrate the total cost at both installation and operation stages, the capital cost can be converted to a daily basis. The objective function of the proposed BES optimal planning model includes three items: the first item C_{inv} refers to the investment cost per-day; the second item C_{opm} refers to daily operation &maintenance cost for BES; and the third item $C_{\mathrm{o},\zeta}$ refers to the expected daily operation cost, as shown in the following equation:

$$\mathrm{Min}\,.\,f = \left(C_{\mathrm{inv}} + C_{\mathrm{opm}}\right) + \mathrm{Exp}\left(\sum C_{\mathrm{o},\zeta}\right) \tag{4}$$

The daily investment cost C_{inv} depends on the installed BES capacity, as shown in the following equation:

$$C_{\mathrm{inv}} = \frac{C_{\mathrm{E}}E_{\mathrm{r}}}{365} \times \left(\frac{d(1+d)^{N_{\mathrm{r}}}}{(1+d)^{N_{\mathrm{r}}+1} - 1}\right) \tag{5}$$

where C_{E} and E_{r} denote the capital cost of BES per unit and energy rating capability of battery, respectively. d and N_{r} denote the interest rate and project year, respectively.

The second term C_{opm} of (4) denotes the daily operation & maintenance cost which is proportionate to the energy capacity of BES, shown as the following equation:

$$C_{\mathrm{opm}} = \sum C_{\mathrm{O}}E_{\mathrm{r}} \tag{6}$$

where C_{O} refers to the daily operation & maintenance cost of BES per unit.

The BES planning problem is constraint by BES investment budget and the location constraint

$$C_{\mathrm{E}}E_{\mathrm{r}} \le \mathrm{CAP} \tag{7}$$

$$L_{\mathrm{bat}} \in \Phi \tag{8}$$

where L_{bat} and Φ denote the possible location of the BES and the set of all the buses, respectively; CAP denotes the investment budget for BES planning.

Given a candidate planning solution, the charging/discharging power of BES, power bought from external substation can be obtained on an hourly basis. Thus, the daily operation cost under all the scenarios can be calculated then. Note that the daily operation cost is considered in this paper in order for a comprehensive cost–benefit analysis. The detailed expression of expected daily operation cost is shown in the following equation:

$$C_{\text{o},\zeta} = \text{Exp}\left(\sum_{\zeta}\sum_{t=1}^{T}\left(C_{\text{buy}} + C_{\text{loss}} + C_{\text{depre}}\right)\right) \tag{9}$$

where ζ denotes the index of different uncertain scenarios, which refers to different load composition and will be discussed in Section 3.3.C_{buy} is the cost of purchasing power from the external grid; C_{loss} is the power loss cost; C_{depre} is the cost of depression of battery lifetime; T and Δt denote the total time horizon and time interval, respectively. Detail cost functions are expressed in the following equations:

$$C_{\text{buy}} = \sum_{t=1}^{T} MP_t P_{\text{buy},t}^{\zeta} \tag{10}$$

$$C_{\text{loss}} = \sum_{t=1}^{T} \eta_{\text{loss}} P_{\text{loss},t}^{\zeta} \tag{11}$$

$$C_{\text{depre}} = \sum_{t=1}^{T} \delta\cdot\left(\left|P_{\text{ch/dis},t}^{\zeta}\right| + E_{\text{BESS},t}^{\zeta}\cdot\eta_l\cdot\Delta t\right) \tag{12}$$

where

$$P_{\text{load},t}^{\zeta} = \sum P_{li,t}^{\zeta} \tag{13}$$

$$P_{\text{loss},t}^{\zeta} = \sum_{i\in\Phi}\sum_{j\in\Phi}\Delta v_{ij}^2\frac{r_{ij}}{x_{ij}^2} \tag{14}$$

In this work, MP_t and $P_{\text{buy},t}^{\zeta}$ denote the time-varying electricity price and power bought from the external grid at time t in scenario ζ. $P_{\text{load},t}^{\zeta}$ and $P_{\text{loss},t}^{\zeta}$ denote total active load demand and power loss at time $t$in scenario ζ after BES installation, respectively. $E_{\text{BESS},t}^{\zeta}$ denotes the energy stored in the battery at time t in scenario ζ; $P_{\text{ch},t}^{\zeta}$ and $P_{\text{dis},t}^{\zeta}$ denote the charging and discharging powers of BES at time t in scenario ζ, respectively. η_l refers to the leakage loss factor of BES, which is calculated based on the battery self-discharge rate. δ refers to the cost coefficient of the battery lifetime depression. r_{ij} and x_{ij} denote the resistance and reactance between lines i and j, respectively, and Δv_{ij} denotes the voltage drop between buses i and j.

It should be noticed that the battery depression cost is calculated based on the total energy usage. According to the impacts of discharge rate on battery life in [8], the total energy usage of battery is remained stable within the reasonable depth of discharge (DOD), e.g. 70%. Thus, the value of δ can be presented as

$$\delta = \frac{C_{\text{inv}}}{E_{\text{r}}\cdot(\text{Life cycle})} \tag{15}$$

3.2 Constraints

The daily scheduling problem is subjected to the following system constraints:

(1) Active/reactive power balance constraint: (see (16)) where $P_{\text{w},t}^{\zeta}$ and $P_{\text{pv},t}^{\zeta}$ denote the wind and solar power outputs at time t in scenario ζ, respectively. $\boldsymbol{G}_{ij}$ and $\boldsymbol{B}_{ij}$ denote the conductance and susceptance matrices between buses i and j, respectively, θ_{ij} denotes the phase angle between buses i and j.

(2) System operation constraint:

- *Voltage constraint:*

$$v^{\min} \le v_{i,t}^{\zeta} \le v^{\max} \tag{17}$$

  where $v_{i,t}^{\zeta}$ denotes the voltage magnitude of bus i at time t in scenario ζ; $v^{\max}$ and $v^{\min}$ denote the maximum and minimum ranges of voltage profile, respectively.
- *Reverse power flow constraint:* In order to avoid interference on the relay-protections and/or potential voltage raising problems, reverse power injection from the distribution network into the upper-level substation is restricted. The following constraint is used to avoid reverse power flow:

$$0 \le S_t^{\zeta} \le S_{g,\text{rated}}^{\max} \tag{18}$$

  where S_t^{ζ} and $S_{g,\text{rated}}^{\max}$ denote the upper-level substation's active power at time t in scenario ζ and the substation's rating capacity, respectively. In practice, where there is excessive renewable power generation and the BES is full, the power curtailment of the renewables will be needed.

(3) BES constraint: In this work, we assume that only the renewable power generation is used to charge the BES. Besides, the reactive power output of batteries is not considered. The battery power transition function is shown as the following equation:

$$E_{\text{BESS},t+1}^{\zeta} = \sum_{t=1}^{T}\left(E_0 + \Delta t\cdot P_{\text{BESS},t}^{\zeta} - |P_{\text{BESS},t}^{\zeta}|\cdot\eta_{\text{c}}\cdot\Delta t - E_{\text{BESS},t}^{\zeta}\cdot\eta_{\text{l}}\cdot\Delta t\right) \tag{19}$$

where η_{c} denotes the charging/discharging loss of BES. Moreover, to ensure that the energy stored in battery satisfy the following day's requirements, a constraint is imposed to make sure that the energy at the end of each scenario equals to the initial energy

$$E(T) = E(0) \tag{20}$$

where $E(0)$ and $E(T)$ denote the initial and final energies stored in the battery, respectively. Also, in this paper, we assume that the batteries should be fully charged and discharged only once in each day due to the lifecycle limitations.

The state-of-charge (SOC) of battery at time t in scenario ζ is expressed as follows:

$$\text{SOC}_t^{\zeta} = E_{\text{BESS},t}^{\zeta}/E_{\text{r}} \tag{21}$$

The main battery operation constraints are shown in (22) and (23):

- *BES power limits:*

$$\begin{cases} P_{\text{w},t}^{\zeta} + P_{\text{pv},t}^{\zeta} + P_{\text{buy},t}^{\zeta} + P_{\text{ch/dis},t}^{\zeta} - P_{\text{load},t}^{\zeta} = v_i\sum v_i\left(G_{ij}\cos\theta + B_{ij}\sin\theta_{ij}\right) \\ Q_{Ci}^{\zeta} - Ql_i = v_i\sum v_i\left(G_{ij}\sin\theta - B_{ij}\cos\theta_{ij}\right) \end{cases} \tag{16}$$

$$0 < \left| P^{\zeta}_{\mathrm{ch/dis},t} \right| \le P^{\mathrm{Max}}_{\mathrm{BESS}} \tag{22}$$

where $P^{\mathrm{Max}}_{\mathrm{BESS}}$ denotes the maximum charging/discharging power of BES units.

- *BES capacity limits:*

$$0 < E^{\zeta}_{\mathrm{BESS},t} < E_{\mathrm{r}} \tag{23}$$

(4) Wind power output constraint:

$$0 \le P^{\zeta}_{\mathrm{w},t} \le P_{\mathrm{w,rated}} \tag{24}$$

(5) Solar power output constraint:

$$0 \le P^{\zeta}_{\mathrm{pv},t} \le P_{\mathrm{pv,rated}} \tag{25}$$

where $P_{\mathrm{w,rated}}$ and $P_{\mathrm{pv,rated}}$ denote the rated output powers of wind turbine and PV panels, respectively.

(6) Capacitor bank constraint

$$\sum Q^{\zeta}_{\mathrm{C}i,t} \le \sum Ql_i \tag{26}$$

where $Q^{\zeta}_{\mathrm{C}i,t}$ denotes the reactive power compensation of the ith capacitor. This constraint was added to ensure that the reactive power provided by capacitor banks does not exceed the required power of the whole system.

(7) Transformer tapping constraint

$$\mathrm{Tap}^{\min} \le \mathrm{Tap}_{\mathrm{tr},t} \le \mathrm{Tap}^{\max} \tag{27}$$

where $\mathrm{Tap}_{\mathrm{tr},t}$ denotes the tap position of OLTC, $\mathrm{Tap}^{\min}$ and $\mathrm{Tap}^{\max}$ denote the minimum and maximum tap positions of OLTC, respectively.

3.3 Chance constraint for CVR target

The deviation of CVR test results in different regions indicates that CVR effects largely rely on the network topology and load compositions. From Table 1, we can easily conclude that more energy savings can be reached if commercial load occupies a large proportion of total system loads. Most previous works assume a uniform load type along each distribution feeder while the diversity of load composition is ignored. In practise, the load composition may experience stochastic change from time to time. Hence, using the single load scenario may significantly downgrade the accuracy of the proposed method. In order to effectively evaluate the impacts of CVR on different load compositions, in this paper a stochastic method is adopted for multiple load composition scenarios.

Specifically, we assume that the total amount of all the loads is fixed, while the exact proportion of each load type is uncertain. As mentioned before, the load types are categorised as residential, industrial and commercial. In this context: Let N_A denotes the total number of distribution loads. The specific amounts of residential, industrial, commercial loads are denoted as N_{Re}, N_{In}, N_{Co}, respectively. The following condition is satisfied:

$$\begin{cases} N_{\mathrm{Re}} + N_{\mathrm{In}} + N_{\mathrm{Co}} = N_A \\ N_{\mathrm{Re}} \in F_{\mathrm{Re}},\ N_{\mathrm{In}} \in F_{\mathrm{In}},\ N_{\mathrm{Co}} \in F_{\mathrm{Co}} \end{cases} \tag{28}$$

where F_{Re}, F_{In}, F_{Co} denote the probability distribution of N_{Re}, N_{In}, N_{Co}, respectively, that can be represented using the normal distribution. According to the load proportion scheme in [16], the mean and variance of N_{Re} are set to be $0.65N_A$ and 0.08, respectively; and the mean and variance of N_{In} are set to be $0.1N_A$ and 0.1, respectively; and the mean and variance of N_{Co} are set to be $0.25N_A$ and 0.1, respectively.

Based on the above assumptions, S different scenarios are randomly generated to represent different load compositions using the Monte Carlo simulation method, each with equal probability. Each scenario ζ is a realisation of different load type distribution. Moreover, a chance constraint is employed to ensure that there is at least $1-\beta$ chance that the percentage of total energy-saving is larger than or equal to α:

$$\Pr\left(\sum_{\zeta=1}^{S} \sum_{t=1}^{T} \Delta E\% \ge \alpha \right) \ge 1-\beta \tag{29}$$

where ζ and S denote the index and total number of all the scenarios, respectively. β is the pre-defined chance constraint confidence level value.

Equation (29) ensures that the CVR implementation should achieve a targeted energy saving level for a certain probability under the stochastic load composition situation.

3.4 Power flow computation with exponential load model

Since the exponential load model is applied, the load power demand is no longer constant but a variable depending on the voltage magnitudes after CVR. Once the voltage changes, the load profiles change along with voltage profiles, which will inevitably induce the changes in power flow calculation. Thus a recursive process must be repeated in power flow calculation. In this paper, the power flow calculation runs iteratively until a pre-defined stopping criterion is satisfied (e.g. the load profiles does not change anymore).

4 Simulation results

The proposed BES planning method was tested on a modified IEEE 15-bus and a 43-bus distribution network systems, respectively. The Monte Carlo embedded differential evolutionary (DE) algorithm is adopted to solve the optimisation problem (4)–(28). The detailed principles of DE can be found in [25]. The experiments were executed on a Dell PC by Matlab (version R2017a).

The hourly solar power outputs and wind speeds in four typical days representing four seasons are obtained from [26, 27], and shown in Figs. 1*a* and *b*, respectively. We can find that the wind power starts to rise at 4:00 am, and maintains high wind speed during 4:00 to 8:00 in the early morning, then goes through a drop in the midday before rising up in midnight. Meanwhile solar power peaks around 10:00–14:00 in the morning, and drops in the night, which is complementary to wind power. Besides, the wind and solar power all exhibit strong seasonal characteristics. For example, wind turbines produce more power in winter while the solar panels generate more power in summer than other seasons. The renewable energy penetration level is set as 30% of the system's total load demand.

Hourly load demand curves in weekdays and weekends are shown in Figs. 2*a* and *b*, respectively. In this paper, the dynamic electricity pricing is considered, and the time-varying market prices for purchasing energy from the external grid are obtained from [6], and shown in Table 2. Comparing to other battery technologies, zinc/bromine (Zn/Br) batteries have many advantages such as high energy density and scalable capacity. Hence Zn/Br technology is chosen in this study. Generally, the power rating is proportional to energy capacity of Zn/Br battery. In this work, we assume P_{BESS} equals to a fifth of the total amount of E_{r} technical and economical properties of Zn/Br are presented in Table 3 [28].

In this work, the total number of scenarios S is set to 1000. As mentioned before, the implementing of CVR leads to 2–5% load reduction effects under most cases [11, 15]. Hence in this work, we set the value of α and β as 2% and 0.1 to ensure there is at least $1-\beta$ chance (90%) that the energy saving effects are larger or equal to 2% of total load demand. However, other values can also be considered depending on practical needs.

4.1 Case 1: 15-bus distribution system

The topology of the 15-bus distribution system with renewable energy resources is shown in Fig. 3, obtained from [8]. The substation transformer is with ±5 tap range and 10 tap positions, in

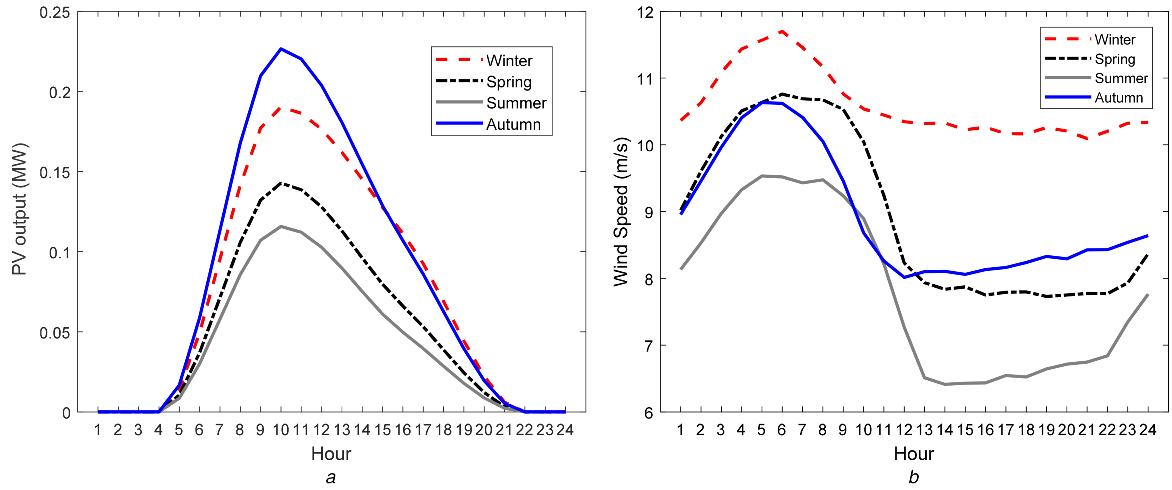

Fig. 1 *Hourly PV output power and wind speed of four seasons*
(a) Hourly PV output power of four seasons, ***(b)*** Hourly wind speed of four seasons

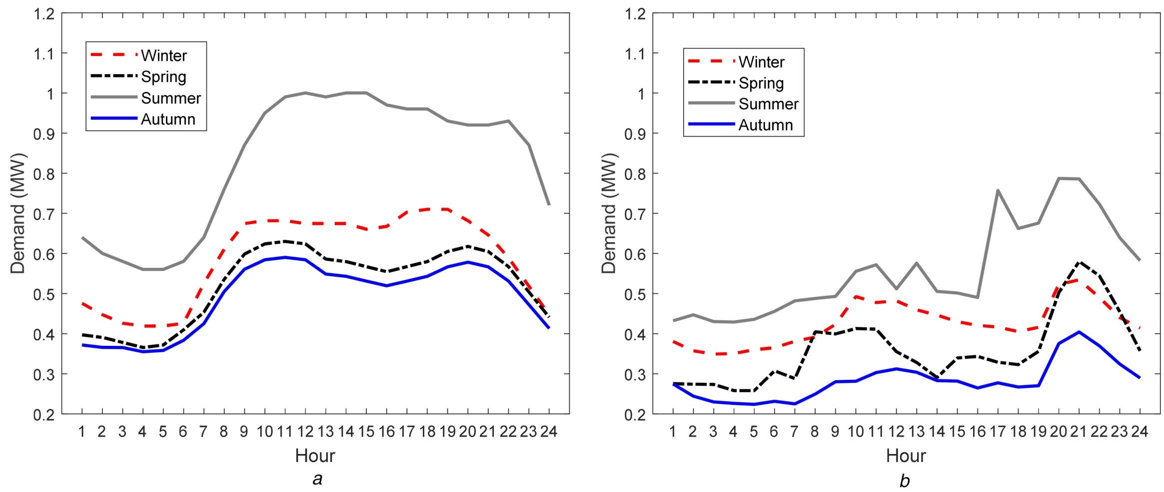

Fig. 2 *Hourly load profiles of four seasons*
(a) Workdays, ***(b)*** Weekends

Table 2 Time-varying market price of upstream grid

Hour	Price, $/kWh	Hour	Price, $/kWh	Hour	Price, $/kWh	Hour	Price, $/kWh
1	0.11	7	0.13	13	0.40	19	0.30
2	0.10	8	0.15	14	0.50	20	0.26
3	0.11	9	0.26	15	0.30	21	0.15
4	0.09	10	0.30	16	0.30	22	0.13
5	0.11	11	0.35	17	0.40	23	0.10
6	0.11	12	0.40	18	0.50	24	0.11

Table 3 Parameters of Zn/Br battery technology

Parameter	Value
unit cost for power rating	225 $/kWh
fixed O&M cost	20$ per day
life cycle	2000 times
round-trip efficiency	60–75%
self-discharge	0.24% [%Energy/day]
SOC limits	20–80%
initial SOC status	20%
investment budget	80,000$
project period	10 years
interest rate	7%

steps of $\Delta tap = 0.01$ p.u. One wind farm is installed at bus 11, and one solar array is located at bus 14, respectively. The wind farm consists of two identical Vestas V52-850kW wind turbines, where the cut-in, cut-out and rated speeds are 4, 25 and 17 m/s, respectively. Two switched capacitor banks are installed at buses 10 and 15, respectively, each is 50 kvar. The allowable voltage range for system operator is set as [0.94, 1.06] p.u.

In order to fully analyse the CVR effect, we simulate the system operation without CVR implementation as a base case for comparison. Table 4 shows the detailed battery planning solutions considering fixed/stochastic load types. Figs. 4*a* and *b* compare the total active load demand consumption in winter scenario with fixed load type under different load profiles for the base case. It is evident that the load profiles reduced significantly during 2:00–7:00 in the morning, and 13:00–20:00 in the afternoon. The load reduction trend remains consistent under different load demand scenarios.

The voltage profiles for all distribution feeders at 18:00 pm in a winter day under fixed load type with/without CVR implement are shown in Fig. 5. It is evident that the voltage profiles along all the distribution feeders decline to a certain extent. The maximum

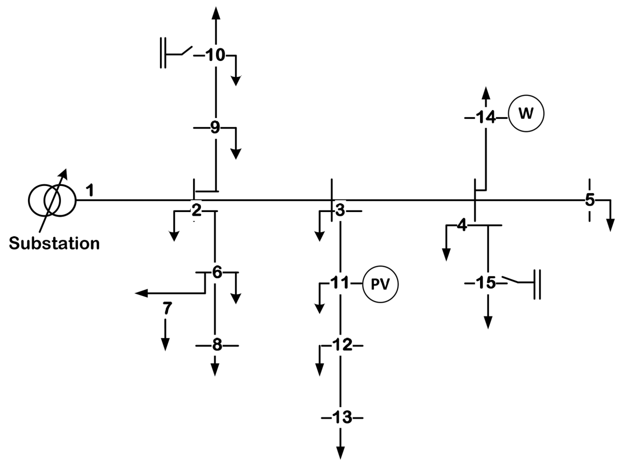

Fig. 3 *Modified IEEE 15-bus distribution radial system*

Table 4a *Continued*

Location	4	7	13
Results under fixed load composition			
size, MWh	0.51	0.55	0.66
total cost per day, $		3823	

Table 4b BES allocation scheme

Location	6	7	13
Results under stochastic load composition			
size, MWh	0.53	0.51	0.71
total cost per day, $		3789	

voltage reduces from 1.04 to 1.035 p.u. on bus 3; meanwhile, the minimum voltage reduces from 1.023 to 1.006 p.u. on bus 13.

Fig. 6 shows the SOC profile with BES installation in a winter day under fixed load type situation. It is evident that the charge/discharge cycles of batteries were largely determined by the time-varying electricity price.

Table 5 summaries the comparison of operation performance per day under base case, fixed/stochastic load compositions, respectively. The maximum CVR factor under two types of load composition scenarios is given as well. The average load consumptions reduced 2.47 and 3.04% under fixed and stochastic load type, respectively. It can be seen that the operation cost is relatively lower when stochastic load composition is considered; meanwhile, the CVR factor is larger. The energy saving target can be satisfied under most scenarios. It is worth mentioning that the CVR factors are higher in the peak load scenario (summer/winter

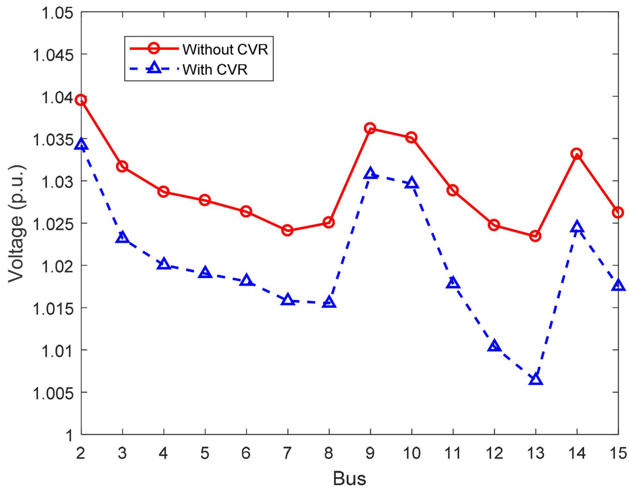

Fig. 5 *Voltage profiles at hour 18:00*

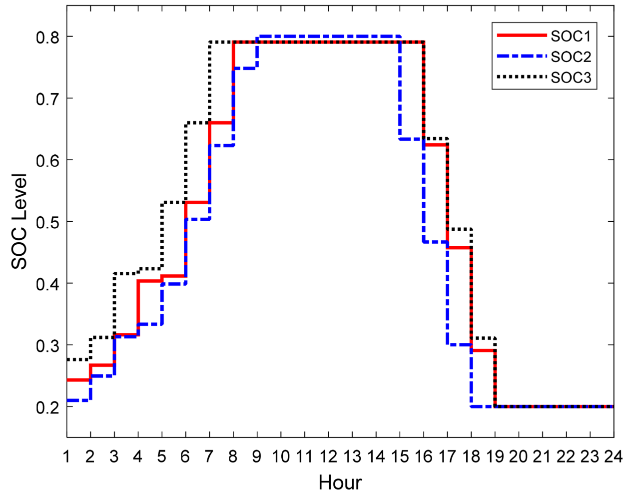

Fig. 6 *SOC profiles for BES units*

scenario). As a result, in ADN the battery storage units are appropriate for voltage regulation.

4.2 Case 2: 43-bus system

In the second case, a 43-radial distribution network is used to testify the effectiveness of proposed method. The substation transformer presents the same characteristics with case 1. Four switched capacitor banks are installed at buses 11, 17, 25 and 33 with 80 kvar, respectively.

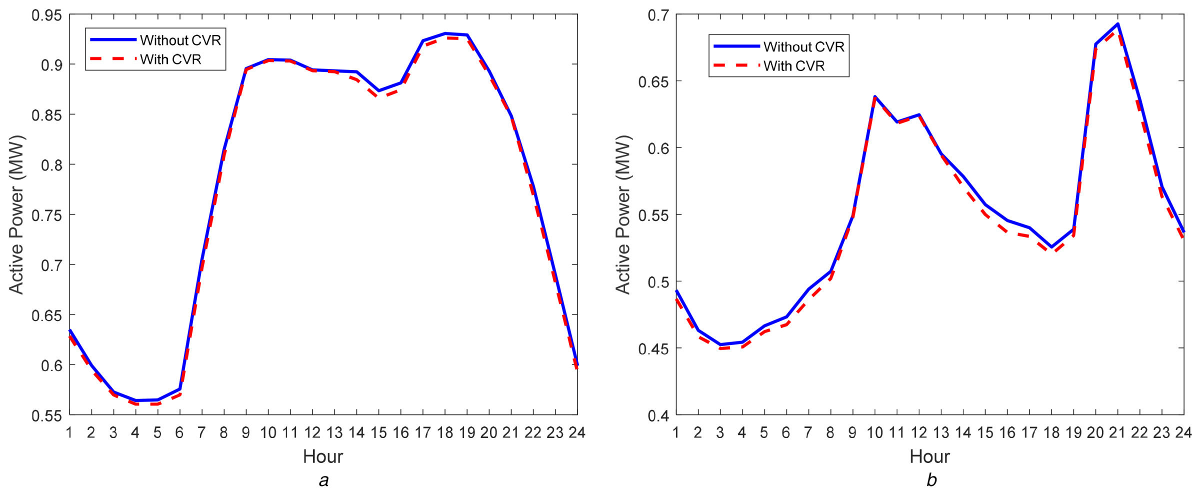

Fig. 4 *Active load demand profiles for the 15-bus system in winter day*
(a) Workdays, ***(b)*** Weekends

Table 5 Operation results comparison

Case	Base	Fixed	Stochastic
average operation cost, $	2932	2786	2763
average power loss, MW	0.90	0.89	0.88
average load consumption, MW	17.58	17.16	17.14
V_{min}, p.u.	1.023	1.006	1.012
average CVR factor	—	1.16	1.18

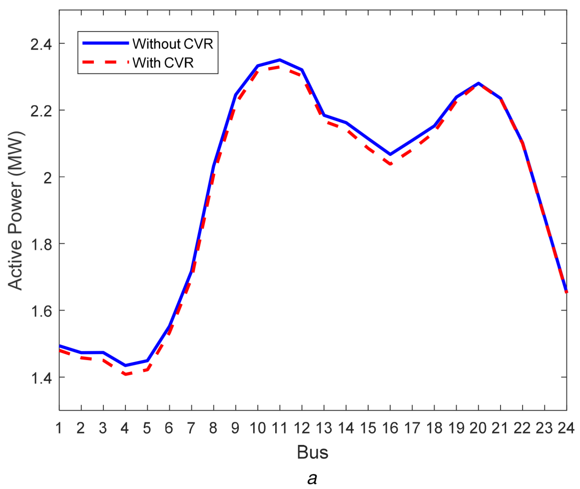

Fig. 7 *Active power profiles for the 43-bus system*
(a) Workdays, ***(b)*** Weekends

Table 6a *Continued*

Location	8	18	25	28	34	37	41
Results under fixed load composition							
size, MWh	0.52	0.55	0.53	0.52	0.51	0.52	0.52
total cost, $/day				11,639			

Table 6b BES allocation scheme

Location	4	18	13	26	33	36	40
Results under stochastic load composition							
size, MWh	0.53	0.50	0.54	0.67	0.52	0.52	0.56
total cost, $/day				11,713			

Table 7 Operation results comparison

Case	Base	Fixed	Stochastic
average operation cost, $	11,176	10,054	9983
average power loss, MW	2.52	2.50	2.48
average load consumption, MW	52.13	50.62	50.25
V_{min} p.u.	1.00	0.981	0.981
average CVR factor	—	1.08	1.09

Figs. 7*a* and *b* compare the active load consumption in summer day with fixed load type considering different load demand profiles. The load consumption reduction trend is very similar to the case 1.

Similarly, the battery allocation plans considering fixed/stochastic load composition situation and the results comparison are shown in Tables 6 and 7, respectively.

From Tables 6 and 7, we find that the average load demand reduction achieves 2.55 and 3.01% under fixed and stochastic load type, respectively. The CVR factor for active power reduction exceeds 1.08 in both cases. Also, the power loss is reduced to some degree. The overall results lead to a conclusion that the implement of CVR will effectively reduce the load demand consumption thus increase energy saving for the utility.

Fig. 8 gives the detail illustration of voltage reduction in each bus at 12:00 am with/without CVR implementation. Similarly, we can find that the maximum voltage reduces from 1.052 to 1.051 p.u. on bus 10; while the minimum voltage reduces from 1.009 to 0.9819 p.u. on bus 41. It should be noticed that the voltage profiles drop further in bus 26-bus 30, bus 38-bus42. The possible explanations are that more batteries are installed along these feeders.

5 Conclusions and future work

This paper proposes an optimal BES planning method considering the combined effects of CVR and BES. The BES placement is defined as a stochastic optimisation problem through the modelling of different load compositions. Moreover, the chance constraint is applied to guarantee the CVR implementation efficiency.

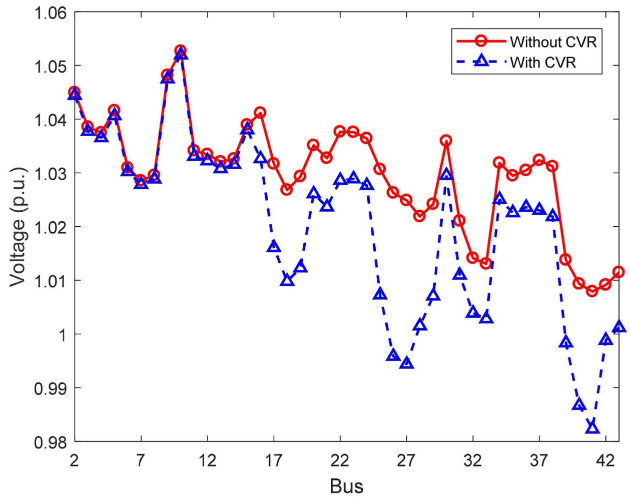

Fig. 8 *Bus voltage profiles at 9:00 for the 43-bus system*

The planning results show that significant power reduction can be achieved by implementing CVR on BES. Specifically, 2% load demand reduction can be achieved in most cases, which indicates that BES is suitable for voltage regulation. Combining CVR and battery would achieve more energy saving for the utility thus help system operator to relieve the stress of load demand growth.

Besides, for high-renewable penetrated distribution networks, the DG inverters have shown great potential for voltage regulation support [29]. In the future, the proposed planning framework can be expanded to include the reactive power output of inverters of the BES for voltage regulation as well. Moreover, other distributed generation resources, capacitor-banks and OLTC can also be employed for voltage regulation in the objective function. Future work also includes the co-planning of DGs, capacitor-banks and other reactive power resources in ADN to analysis the coordinated optimisation effects of CVR implementation.

6 Acknowledgments

Yan Xu's work is supported by Nanyang Assistant Professorship from Nanyang Technological University, Singapore. This work is also supported in part by the National Natural Science Foundation of China under Grant 71331001 and 71420107027; in part by the ARC Discovery Grant (DP170103427); and in part by the 2015 Science and Technology Project of China Southern Power Grid (WYKJ00000027).

7 References

[1] Pilo, F., Jupe, S., Silvestro, F., , *et al.*: 'Planning and optimization methods for active distribution systems'. WG C6.19: TB 591, CIGRE, Paris, France, 2014

[2] Zhang, C., Xu, Y., Dong, Z.Y., *et al.*: 'Robust operation of microgrids via two-stage coordinated energy storage and direct load control', *IEEE Trans. Power Syst.*, 2017, **32**, (4), pp. 2858–2868

[3] Awad, A.S.A., El-Fouly, T.H.M., Salama, M.M.A.: 'Optimal ESS allocation for load management application', *IEEE Trans. Power Syst.*, 2015, **30**, (1), pp. 327–336

[4] Bahramirad, S., Reder, W., Khodaei, A.: 'Reliability-constrained optimal sizing of energy storage system in a microgrid', *IEEE Trans. Smart Grid*, 2012, **3**, (4), pp. 2056–2062

[5] Nick, M., Hohmann, M., Cherkaoui, R., *et al.*: 'Optimal location and sizing of distributed storage systems in active distribution networks'. Power Tech (POWERTECH), 2013, Grenoble, 2013, pp. 1–6

[6] Chen, S., Gooi, H.B., Wang, M.: 'Sizing of energy storage for microgrids', *IEEE Trans. Smart Grid*, 2012, **3**, (1), pp. 142–151

[7] Luo, F., Meng, K., Dong, Z.Y., *et al.*: 'Coordinated operational planning for wind farm with battery energy storage system', *IEEE Trans. Sustain. Energy*, 2015, **6**, (1), pp. 253–262

[8] Zhang, Y., Dong, Z.Y., Luo, F., *et al.*: 'Optimal allocation of battery energy storage systems in distribution networks with high wind power penetration', *IET Renew. Power Gener.*, 2016, **10**, (8), pp. 1105–1113

[9] Preiss, R., Warnock, V.: 'Impact of voltage reduction on energy and demand', *IEEE Trans. Power Appar. Syst.*, 1978, **5**, (6), pp. 1665–1671

[10] Electrical Transmission and Distribution, *Reference Book* (PA: Westinghouse Electric Corp., Pittsburgh, 5th edn.), pp. 666–716

[11] Bokhari, A., Raza, A., Diaz-Aguilo, M., *et al.*: 'Combined effect of CVR and DG penetration in the voltage profile of low-voltage secondary distribution networks', *IEEE Trans. Power Deliv.*, 2016, **31**, (1), pp. 286–293

[12] Jauch, E.T.: 'Volt/var management? An essential 'SMART' function'. Power Systems Conf. and Exposition, 2009, PSCE'09, IEEE/PES, 2009, pp. 1–7

[13] Fuller, J., Tuffner, F., Schneider, K., *et al.*: 'Evaluation of conservation voltage reduction (CVR) on a national level'. DE-AC05-76RL01830, Pacific Northwest National Laboratory, United States Department of Energy, July 2010

[14] Lefebvre, S., Gaba, G., Ba, A.O., *et al.*: 'Measuring the efficiency of voltage reduction at Hydro-Qubec distribution'. Proc. of Power and Energy Society General Meeting-Conversion and Delivery of Electrical Energy in the 21st Century IEEE, 2008, pp. 1–7

[15] Ellens, W., Berry, A., West, S.: 'A quantification of the energy savings by conservation voltage reduction'. 2012 IEEE Int. Conf. Power System Technology (POWERCON), 2012, pp. 1–6

[16] Padilha-Feltrin, A., Rodezno, D.A.Q., Mantovani, J.R.S.: 'Volt-VAR multiobjective optimization to peak-load relief and energy efficiency in distribution networks', *IEEE Trans. Power Deliv.*, 2015, **30**, (2), pp. 618–626

[17] Zhaoyu, W., Bokan, C., Jianhui, W., *et al.*: 'Stochastic DG placement for conservation voltage reduction based on multiple replications procedure', *IEEE Trans. Power Deliv.*, 2015, **30**, (3), pp. 1039–1047

[18] Quijano, D.A., Feltrin, A.P.: 'Assessment of conservation voltage reduction effects in networks with distributed generators'. 2015 IEEE PES Innovative Smart Grid Technologies Latin America (ISGT LATAM), 2015, pp. 393–398

[19] Kennedy, B.W., Fletcher, R.: 'Conservation voltage reduction (CVR) at Snohomish county PUD', *IEEE Trans. Power Syst.*, 1991, **6**, (3), pp. 986–998

[20] IEEE 1250-1995-(ANSI): 'IEEE Guide for Service to Equipment sensitive to Momentary Voltage Disturbances'.

[21] ANSI: 'ANSI Standard C84.1-1995 Electric Power Systems and Equipment Voltage Ratings (60 Hz)'. 1995

[22] Relaying, P.: '*Electricity Distribution Network Design*' (Power Engineering Review, 1996)

[23] 'Battery Energy Storage technologies for power system'. IPHE workshop on Hydrogen – A Competitive Energy Storage Medium to Enable the Large Scale Integration of Renewable Energies, Seville, Spain, November 2012

[24] Caetano, W., Jota, P., Goncalves, E.: 'Comparison between static models of commercial/residential loads and their effects on conservation voltage reduction'. 2013 IEEE Int. Conf. Proc. Smart Energy Grid Engineering (SEGE), August 2013, pp. 1–6

[25] Wong, K.P., Dong, Z.Y.: '*Differential evolution, an alternative approach to evolutionary algorithm, invited book chapter in modern heuristic optimization: theory and applications to power systems*' (John Wiley &Sons, Ltd, New York, 2007), pp. 171–187

[26] Australia's official weather forecast & weather radar website. Available at http://www.bom.gov.au/

[27] CISLResearchDataArchive. Available at: http://rda.ecar.edu/

[28] Wang, Z., Wang, J.: 'Time-varying stochastic assessment of conservation voltage reduction based on load modeling', *IEEE Trans. Power Syst.*, 2014, **29**, (5), pp. 2321–2328

[29] Xu, Y., Dong, Z.Y., Zhang, R., *et al.*: 'Multi-timescale coordinated voltage/var control of high renewable-penetrated distribution networks', *IEEE Trans. Power Syst.*, 2017, **99**, (99), pp. 1–1, DOI: 10.1109/TPWRS.2017.2669343

8 Appendix

8.1 Appendix 1: IEEE 15-bus distribution test system

See Table 8.

8.2 Appendix 2: 43-bus distribution test system

See Table 9.

Table 8 IEEE 15-bus distribution test system

Line section			R, p.u.	X, p.u.
No.	Send. end	Recv. end		
1	1	2	0.000541	0.000529
2	2	3	0.000468	0.000458
3	3	4	0.000336	0.000329
4	4	5	0.000609	0.000411
5	2	9	0.000805	0.000543
6	9	10	0.000675	0.000455
7	2	6	0.001023	0.000690
8	6	7	0.000435	0.000294
9	6	8	0.000501	0.000354
10	3	11	0.000718	0.000484
11	11	12	0.000979	0.000661
12	12	13	0.000805	0.000543
13	4	14	0.000892	0.000752
14	4	15	0.000479	0.000404

Table 9 43-bus distribution test system

	Line section		R	X
No.	Send. end	Recv. end	(p.u.)	(p.u.)
1	1	2	0.000270618	0.000264698
2	2	3	0.000234048	0.000228928
3	3	4	0.000168222	0.000164542
4	4	5	0.000304696	0.00020552
5	2	9	0.000402634	0.00027158
6	9	10	0.000337342	0.00022754
7	2	6	0.000511454	0.00034498
8	6	7	0.00021764	0.0001468
9	6	8	0.000250286	0.00017682
10	3	11	0.000359106	0.00024222
11	11	12	0.00048969	0.00033030
12	12	13	0.000402634	0.000271580
13	4	14	0.000446162	0.000300940
14	4	15	0.000239404	0.000161480
15	1	16	0.000270618	0.000264698
16	16	17	0.000234048	0.0002289280
17	17	18	0.000168222	0.0001645420
18	18	19	0.0003046960	0.0002055200
19	16	23	0.0004026340	0.0002715800
20	23	24	0.0003373420	0.0002275400
21	16	20	0.0005114540	0.0003449800
22	20	21	0.0002176400	0.0001468000
23	20	22	0.0002502860	0.0001768200
24	17	25	0.0003591060	0.0002422200
25	25	26	0.0004896900	0.0003303000
26	26	27	0.0004026340	0.0002715800
27	18	28	0.0004461620	0.0003009400
28	18	29	0.0002394040	0.0001614800
29	16	23	0.0002706180	0.0002646980
30	23	24	0.0002340480	0.0002289280
31	16	20	0.0001682220	0.0001645420
32	20	21	0.0003046960	0.0002055200
33	20	22	0.0004026340	0.0002715800
34	17	25	0.0003373420	0.0002275400
35	25	26	0.0005114540	0.0003449800
36	26	27	0.0002176400	0.0001468000
37	18	28	0.0002502860	0.0001768200
38	18	29	0.0003591060	0.0002422200
39	1	30	0.0004896900	0.0003303000
40	30	31	0.0004026340	0.0002715800
41	31	32	0.0004461620	0.0003009400
42	32	33	0.0002394040	0.0001614800
43	30	37	0.0002340480	0.0002289280
44	37	38	0.0001682220	0.0001645420